

Dynamical phenomena in Fibonacci semiconductor superlattices

Enrique Diez,^{1,2,†} Francisco Domínguez-Adame,^{2,3,4,‡} Enrique Maciá,^{2,3,§} and
Angel Sánchez^{1,2,4,*}

¹*Departamento de Matemáticas, Escuela Politécnica Superior,
Universidad Carlos III, E-28911 Leganés, Madrid, Spain*

²*Grupo Interdisciplinar de Sistemas Complicados, Escuela Politécnica Superior,
Universidad Carlos III, E-28911 Leganés, Madrid, Spain*

³*Departamento de Física de Materiales, Facultad de Físicas,
Universidad Complutense, E-28040 Madrid, Spain*

⁴*Theoretical Division and Center for Nonlinear Studies,
Los Alamos National Laboratory, Los Alamos, New Mexico 87545
(December 2, 2021)*

We present a detailed study of the dynamics of electronic wavepackets in Fibonacci semiconductor superlattices, both in flat band conditions and subject to homogeneous electric fields perpendicular to the layers. Coherent propagation of electrons is described by means of a scalar Hamiltonian using the effective-mass approximation. We have found that an initial Gaussian wavepacket is filtered selectively when passing through the superlattice. This means that only those components of the wavepacket whose wavenumber belong to allowed subminibands of the fractal-like energy spectrum can propagate over the entire superlattice. The Fourier pattern of the transmitted part of the wavepacket presents clear evidences of fractality reproducing those of the underlying energy spectrum. This phenomenon persists even in the presence of unintentional disorder due to growth imperfections. Finally, we have demonstrated that periodic coherent-field induced oscillations (Bloch oscillations), which we are able to observe in our simulations of periodic superlattices, are replaced in Fibonacci superlattices by more complex oscillations displaying quasiperiodic signatures, thus shedding more light onto the very peculiar nature of the electronic states in these systems.

PACS number(s): 72.10.-d, 72.15.Rn, 73.20.Dx

I. INTRODUCTION

Since the fabrication of aperiodic semiconductor superlattices (SLs) arranged according to the Fibonacci¹ and Thue-Morse² sequences, there has been a growing interest in their electronic properties, both from experimental³⁻⁸ and theoretical^{4,9-11} viewpoints. One of the most appealing motivation for these studies is the theoretical prediction that ideal aperiodic SLs should exhibit a highly-fragmented electronic spectrum displaying self-similar patterns.^{12,13} And, in fact, photoluminescence excitation spectroscopy at low temperature reveals the existence of a fragmented density of states consistent with theoretical predictions.⁵

Other motivation for the study of dynamical phenomena in aperiodic systems is the following. Electron states in periodic SLs spread uniformly over the whole SL (Bloch states) and the energy spectrum is composed by minibands and minigaps. In the absence of electric field, these extended states are characterized by a transmission probability very close to unity. When a homogeneous electric field is applied perpendicular to the layer plane, electronic states become localized (Stark-Wannier states) and the energy spectrum consists of equally spaced levels (Stark-Wannier ladder). From the perspective of quantum evolution, Bloch states lead to Bloch oscillations (BOs) when the electric is applied.^{14,15} The BO time pe-

riod of the electronic motion in real as well as in k space is given by¹⁵

$$\tau_B = \frac{2\pi\hbar}{eFd}, \quad (1)$$

where d is the SL constant. High-quality SLs make it possible to obtain BO time periods larger than the scattering time for reasonable values of the applied electric field F . Reports of unambiguous experimental evidence for BOs in periodic GaAs-Ga_{1-y}Al_yAs SLs have been recently appeared,^{16,17} using an experimental method previously proposed by von Plessen and Thomas.¹⁸ This picture is assumed to be no longer valid in Fibonacci SLs (FSLs) because in the thermodynamical limit electron states are critical instead of extended in flat band conditions, from a strict mathematical point of view. However, since actual FSLs are of finite size, one could expect similar transport properties (i. e., high transmission coefficient) to that shown by extended electronic states since they spread over the whole FSL, although we insist that they are not Bloch states. Hence the question as to whether BOs will be observed or not in FSL arises quite naturally.

Therefore the aim of this work is twofold. In the first place, we provide a complete characterization of electronic states in FSLs, giving a detailed description of dynamical phenomena of electronic wavepackets, which,

as far as we know, have not been reported in the literature. In this way, we are led to the conclusion that FSLs act as *efficient electronic filters*, an appealing property in order to use them in actual devices of technological interest. In the second place, we investigate the possibility to observe BOs in FSLs, suggesting the convenience of generalizing the concept of periodic BOs to the case of *quasiperiodic* oscillations in order to properly describe the dynamical behavior of critical states under the action of homogeneous electric fields.

To this end, in this paper we address the study of time-dependent effects in FSLs by solving numerically the effective-mass equation for the envelope-function, both in the absence of external fields and under homogeneous electric fields. To be specific, we consider the problem of quantum evolution of electronic wavepackets initially localized in space impinging on the FSL. The wavepacket dynamics will be properly described by means of the time-dependent transmission probability. The transmitted portion of the wavepacket will be characterized by its Fourier transform, aiming to search for particular signatures arising from the scattering event. To get an estimation of the spreading of the wavepacket as a function of time, we will use the time-dependent inverse participation ratio (IPR) as well as the mean-square displacement. Finally, since unintentional imperfections appear during growth in actual FSLs, we have analyzed a modified version of our model to investigate the possible existence of a competition between the long-range quasiperiodic order and the short-range disorder which could be detected by our time analysis.

II. MODEL

We consider quantum-well based GaAs-Ga_{1-y}Al_yAs SLs with the same barrier thickness b in the whole sample. The thickness of each quantum-well is $\Delta x_n - b \equiv x_n - x_{n-1} - b$, x_n being the position of the center of the n th barrier and x the growth direction. We will focus on electronic states close to the bandgap with $\mathbf{k}_\perp = 0$ and neglect nonparabolicity effects hereafter, so that the Ben Daniel-Duke Hamiltonian suffices to describe those states. The envelope-functions for electron wavepackets satisfy the following quantum-evolution equation

$$i\hbar \frac{\partial \Psi(x, t)}{\partial t} = \mathcal{H}(x) \Psi(x, t). \quad (2)$$

The time-independent Hamiltonian $\mathcal{H}(x)$ is given by

$$\mathcal{H}(x) = -\frac{\hbar^2}{2m^*} \frac{d^2}{dx^2} + V_{\text{SL}}(x) - eFx, \quad (3)$$

where $V_{\text{SL}}(x)$ is the SL potential under flat bands condition and F is the electric field. The height of the barrier for electrons is given by the conduction-band offset at the interfaces ΔE_c . We take the origin of electron energies at the GaAs conduction-band edge.

The particular kind of SLs subject of this work, FSLs, can be grown starting from two basic building blocks A and A' by means of molecular beam epitaxy.¹ Here A (A') consists of a quantum-well of thickness a (a') and a barrier of thickness b . The Fibonacci sequence S_n is generated by appending the $n-2$ sequence to the $n-1$ one, i.e., $S_n = S_n S_{n-1}$. This construction algorithm requires initial conditions which are chosen to be $S_0 = A$ and $S_1 = A'$. In this way, finite and self-similar quasiperiodic SLs are obtained by n successive applications of these rules leading to the ordering $A A' A A A' A \dots$, containing $N = F_n$ barriers. The Fibonacci numbers are generated from the recurrence law $F_n = F_{n-1} + F_{n-2}$, starting with $F_0 = F_1 = 1$. A few blocks of the resulting SL potential V_{SL} are shown in Fig. 1.

Unintentional disorder appearing during growth in *actual* SLs depends critically on the growth conditions and it is unknown in most cases. Therefore, one is forced to develop a simple model, making reasonable assumptions on the type of disorder for each particular sample. For instance, islands protruding from one semiconductor into the other cause in-plane disorder and break translational invariance parallel to the heterojunction. If the in-plane average size of these protrusions is much larger than the mean-free-path, then carriers only *see* an ensemble of different layer thicknesses.¹⁹ We model local excess or defect of monolayers by allowing Δx_n to fluctuate uniformly around the nominal values $a+b$ or $a'+b$. For definiteness we take $\Delta x_n = a(1+W\epsilon_n)+b$ or $\Delta x_n = a'(1+W\epsilon_n)+b$, where W is a positive parameter measuring the maximum fluctuation and ϵ_n 's are distributed according to a uniform probability distribution $P(\epsilon_n) = 1$ if $|\epsilon_n| < 1/2$ and zero otherwise. Note that ϵ_n is a random variable, even when the mean values of Δx_n follow the Fibonacci sequence.

III. NUMERICAL ANALYSIS

We study the quantum dynamics of an initial Gaussian wavepacket

$$\Psi(x, 0) = [2\pi(\Delta X)^2]^{-1/4} \exp \left[\frac{ik_0 x - (x - x_0)^2}{4(\Delta X)^2} \right], \quad (4)$$

impinging on the FSL, where the mean kinetic energy is $\langle E \rangle = \hbar^2 k_0^2 / 2m^*$ and ΔX measures the width of the electron wavepacket. The solution of Eq. (2) is given by

$$\Psi(x, t) = \exp \left(\frac{i}{\hbar} \mathcal{H}(x) t \right) \Psi(x, 0). \quad (5)$$

The finite difference representation of the exponential²¹

$$\exp \left(\frac{i}{\hbar} \mathcal{H}(x) t \right) = \frac{1 - \frac{i}{2\hbar} \mathcal{H}(x) \delta t}{1 + \frac{i}{2\hbar} \mathcal{H}(x) \delta t} + \mathcal{O}[(\delta t)^3], \quad (6)$$

where δt is the time step, brings a powerful and high-accurate numerical method. In addition, it ensures probability conservation,²² which has been used at every time step as a first test of the accuracy of results. Boundary conditions read $\Psi(\infty, t) = \Psi(-\infty, t) = 0$ and we have chosen the FSL length sufficiently large to be sure than the wavepacket never comes close to the boundaries.

Transmission properties of the electronic wavepacket can be successfully analyzed by means of the time-dependent transmission probability $P_T(t)$, which is nothing but the probability that at time t the electron is found to have crossed the whole SL,

$$P_T(t) = \int_L^\infty dx |\Psi(x, t)|^2, \quad (7)$$

where L is the length of the system. In addition, to get a complete characterization of the motion of the wavepacket, we use the time-dependent inverse participation ratio, $\text{IPR}(t)$, and the mean-square displacement, $\sigma(t)$. The IPR is defined as

$$\text{IPR}(t) = \int_{-\infty}^\infty dx |\Psi(x, t)|^4, \quad (8)$$

and it gives an estimation of the spatial extent and the degree of localization of electronic wavepackets, which can indeed provide very much information. Delocalized states are expected to present small IPR (in the ballistic limit, without applied field, it vanishes as t^{-1}), while localized states have larger IPR. The mean-square displacement describes how quantum diffusion of wavepackets initially located in the middle of the FSL takes place. The mean-square displacement $\sigma(t)$ is defined as

$$\sigma^2(t) = \int_{-\infty}^\infty (x - \bar{x})^2 |\psi(x, t)|^2 dx. \quad (9)$$

with

$$\bar{x} = \int_{-\infty}^\infty x |\psi(x, t)|^2 dx.$$

In the asymptotic regime ($t \rightarrow \infty$) one expects $\sigma^2(t) \sim t^\gamma$. The exponent is $0 < \gamma < 1$ for localized states, $\gamma = 1$ for ordinary diffusion, $1 < \gamma < 2$ for super-diffusion, and $\gamma = 2$ for ballistic regime.

IV. RESULTS AND DISCUSSIONS

A. Zero field behavior

As a typical SL we have chosen a GaAs-Ga_{0.65}Al_{0.35}As structure, for which the conduction-band offset is $\Delta E_c = 0.25$ eV and the effective-mass is $m^* = 0.067m$, m being the free electron mass. In our computations we have taken $a = b = 32$ Å and $a' = 26$ Å. With our chosen parameters there exists only one miniband below the barrier

in periodic SLs, ranging from 0.102 eV up to 0.177 eV. Thus the miniband width is much larger than the exciton binding energy, which amounts ~ 0.01 eV in the present SLs. This is a relevant fact, for it has been shown that electronic localization (Stark-Wannier states) is suppressed for low miniband widths. Finally, to compare with actual SL's, we have considered the parameter W , which governs the imperfection magnitude, ranging from 0 up to a maximum of 0.05. This value amounts to having protrusions thicknesses of half a monolayer on average.

Figure 2 collects the results of a typical simulation of a wavepacket for a FSL. First, in Fig. 2(a) we show the transmission coefficient, τ , as a function of energy for a perfect ($W = 0$) FSL with $N = 144$ wells, computed by means of the transfer-matrix formalism.²³ The overall structure of the energy spectrum is characterized by the presence of four main subminibands (notice that transmission peaks are clustered around energies ~ 0.120 , 0.155 , 0.175 , and 0.200 eV). An enlarged view of each cluster of peaks shows that the fragmentation pattern follows a trifurcation scheme in which each cluster splits from one to three subclusters upon going to higher-order generations of FSL's. This splitting scheme agrees with that previously reported in FLSs.^{9,24} The main question is to know how this highly-fragmented energy spectrum affects the quantum evolution of a wavepacket incident on the FSL.

Figure 2(a) also shows the Fourier transform of an initial Gaussian wavepacket at $t = 0$ with its average kinetic energy $\langle E \rangle = 0.160$ eV lying in the centermost subminiband and spatial width $\Delta X = 200$ Å. After the transmitted electron is found to have crossed the whole FSL [~ 6 ps, see Fig. 3(a)], the Fourier transform of the electronic wavepacket changes dramatically in perfect FSLs ($W = 0$). Instead of a smooth function, the Fourier transform presents a series of marked peaks. Conspicuously, the energy of these peaks coincides with the higher values of the transmission coefficient, thus indicating that *the FSL acts as an efficient electronic filter*. Notice that the Fourier transform also displays the same splitting pattern than the energy spectrum, being observable even the third level of hierarchy in the upper subminiband. A physical understanding of this behavior is achieved if one considers that the initially localized wavepacket can be regarded as a combination of plane waves in a continuous band. Since the dispersion relation (energy versus wavenumber) is self-similar with a hierarchy of splitted subminibands separated by well-defined minigaps [see the transmission coefficient shown in Fig. 2(a)], only those components whose wavenumber belongs to an allowed subminiband can propagate over large distances and, consequently, contributing to the transmitted part of the wavepacket. What it is most important for practical purposes, we have found that unintentional disorder does not severely affect filtering properties, as shown in Fig. 2(b) for $W = 0.05$. Although an overall reduction of the transmitted components is found, signatures of the above mentioned level splitting are still clearly observed

in the Fourier patten, particularly at the central energy region around 0.155 eV.

Quantum evolution of electronic wavepackets will depend upon the system length since the fragmentation of the energy spectrum is higher on increasing N . Figure 3(a) shows the time-dependent transmission probability as a function of time for perfect ($W = 0$) FSLs of various lengths. For comparison, it should be borne in mind that the transmission probability vanishes in intentionally disordered SLs for moderately large sizes, thus providing further evidences of the differences between random and aperiodic systems. The occurrence of the plateau for larger times indicates that the transmitted wavepacket has crossed the whole FSL. Thus, the larger the FSL length, the later the plateau appears, as was to be expected. Interestingly, the value of the asymptotic probability decreases on increasing the FLS length. This reduction of the transmission probability means that filtering effects are stronger as the fragmentation of the energy spectrum is higher. That is to say, the equivalent miniband-width, defined as the sum of all the allowed subminibands, decreases as a power of N as a consequence of the quasiperiodic topology of the FSL¹¹ and, therefore, more and more components of the wavepacket are back reflected. Figure 3(b) presents the results for the time-dependent transmission probability as a function of time for imperfect ($W = 0.05$) FSLs of various lengths. A comparison with Fig. 3(a) indicates a decrease of the transmission probability since short-range disorder tends to localize particles, according to the Anderson theory. However, this effect is almost unnoticeable for relatively short (say N smaller than 89) FSL, in agreement with our previous estimations based on the study of the equivalent miniband-width.²⁵ Therefore, we are led to the conclusion that moderately large fluctuations cannot destroy filtering effects of actual FSLs and that they can safely be used for practical purposes. The study of the mean-square displacement in perfect and imperfect FSLs provides additional support in this sense. We have placed the initial Gaussian wavepacket in the middle of the FSL, with $\Delta X = 20 \text{ \AA}$ and $\langle E \rangle = 0.160 \text{ eV}$. In all cases we have observed the super-diffusive regime $\sigma^2(t) \sim t^\gamma$ with $\gamma \simeq 1.2$, as illustrated in Fig. 4. This result shows that the time-dependent properties are quite similar for both perfect and imperfect FSLs as large as samples containing $N = 377$ wells. It is also interesting to note that the exponent γ obtained in our study, which is based on a realistic continuous model, is lower than that obtained by considering tight-binding Hamiltonians.²⁶

B. Homogeneous field effects

We now comment on our results when a homogeneous electric field is applied perpendicular to the layers. One expects that BOs are to be observed in periodic SLs in the limit of high electric fields. The localization length of

Stark-Wannier states, the static counterpart of the BOs, is of the order of $\Delta E/eF$, ΔE being the width of the allowed miniband, so that we can roughly estimate that the condition $\Delta E/eF \sim a + b$ establish the high field regime. In our SL this field amounts $F \simeq 100 \text{ kV/cm}$. Figure 5(a) presents the results for the IPR when the initial Gaussian wavepacket with $\Delta X = 20 \text{ \AA}$ and $\langle E \rangle = 0.160 \text{ eV}$ is located in the middle of the periodic SL, the electric field being $F = 100 \text{ kV/cm}$. The IPR displays periodic oscillations with marked peaks at times $t_k = k\tau_B$, where k is any arbitrary, nonnegative integer and $\tau_B = 0.065 \text{ ps}$. Thus the IPR is bounded below, indicating that the wavepacket is localized (dynamical localization) but its spatial extent varies periodically in time. Notice that the value of the oscillation period is in excellent agreement with the theoretical prediction $\tau_B = 2\pi\hbar/(eFd)$ given in (1). It is also worth to mention that the initial state $\Psi(x, 0)$ is not completely restored after each oscillation, as it should be if interband tunneling were negligible.¹⁸ Thus we are led to the conclusion that intraband tunneling plays a role in our periodic SL.

Results corresponding to a FSL with the same initial condition as before are also shown in Fig. 5(a). First of all, we observe that at short times we can detect two oscillations coinciding with the positions of the first two BO peaks, but at larger times *periodic* BOs are completely absent in FSLs. The absence of Bloch oscillations in FSLs simply reflects the fact that their extended states are no longer Bloch states. Bloch states are characterized by a periodic pattern, but this is not the case in the FSL, where critical states spreading over the whole system show quasiperiodic patterns.²⁰ In this sense, signatures of a quasiperiodic oscillation pattern in the IPR corresponding to the FSL can be seen from Fig. 5(a) in the interval $0.5 \leq t \leq 1 \text{ ps}$. To this end, we introduce the ratio p/q , where q is the number of oscillations of the FSL IPR comprised in a given number p of periodic BOs. In this way we obtain the following sequence $p/q = 2/3, 3/5, 2/3, 5/8, 2/3, 7/11, 2/3, \dots$ which converges to $2/3$, an approximant of the inverse golden mean $\tau_G \equiv (\sqrt{5} - 1)/2$.

This facts can be described by means of the following scenario, based on our previous discussion on the localization degree of electronic states under an applied electric field. For such high electric fields the spatial extent of the electronic states is of the order of the SL constant and, consequently, the electron cannot *see* the long-range quasiperiodic potential. In fact, differences between periodic and Fibonacci SLs at short times are actually very small [see Fig. 5(a)]. As soon as some components escapes from the localization region (for instance, those states above the barrier has a high transmission coefficient) the effect of quasiperiodicity takes place. To get further confirmation of this assertion we have also studied the case of lower electric fields, as shown in Fig. 5(b) for $F = 10 \text{ kV/cm}$, when the localization length is about ten SL periods. It becomes apparent that no signatures

of BOs can be detected even at short times. Moreover, Fig. 5(b) also displays the result for the periodic SL and the same electric field. Notice that the initial states is completely restored after each BO, the suggesting that in this regime interband tunneling is actually negligible.

V. CONCLUSION

In this paper we have studied quantum dynamics of wavepackets in Fibonacci SLs. After solving numerically the time-dependent effective-mass equation arising from the Ben Daniel-Duke Hamiltonian, we have found that an initial Gaussian wavepacket undergoes complicate scattering events at the FSL. In particular, the Fourier spectrum of the transmitted part of the wavepacket is no longer smooth but presents many marked peaks. These peaks correspond to the allowed subminibands of the energy spectrum, thus being a clear indication that the FSL acts as a fine electronic filter. Transmission properties under zero bias have also been successfully characterized by means of the transmission probability given by (7). From these results we have learned that unintentional disorder arising during growth have no noticeable effects on the filtering capabilities of short FSLs, because they only cause an overall decrease of the transmitted amplitude. On the other hand, the spatial degree of localization of wavepackets driven by an electric field has been properly described by means of the time-dependent IPR: As a check, in periodic SLs we have obtained the dynamical localization fields as well as BO's. On the contrary, quantum dynamics in FSLs also exhibits dynamical localization although it turns out to be much more intricate. In particular, no evidence of periodic Bloch oscillations was observed. Instead, the very concept of BO should be revisited in order to include the possibility of *quasiperiodic* pattern oscillations emerging from the quasiperiodic nature of the system. This result puts another piece of evidence about the very peculiar nature of electronic states in Fibonacci systems.²⁰

As a concluding remark, we want to stress that with this work we have sufficiently demonstrated the existence of distinct physical observable consequences of singular energy spectra like that of the FSL. For instance, the fragmentation of the SL minibands could serve as the basis for electronic filters, in a similar fashion to metallic Fibonacci multilayers acting as selective filters of soft X-ray radiation.²⁷ It is quite clear that the output of such a device is but an image of its fractal spectrum, which, in turn, is intimately connected with the quasiperiodic nature of the SL and hence with the information it contains. Therefore, aside from the possibility of building the specific filter-like devices we already mentioned, designed with this or other quasiperiodic sequence according to the desired application, it might as well be that this kind of systems can be used in transmitting or processing information. This and other relations already estab-

lished between quasiperiodic nanoelectronic devices and information theory²⁴ pave the way to a very exciting and promising line of cross-disciplinary research.

ACKNOWLEDGMENTS

F. D.-A. and A. S. are thankful to Alan R. Bishop for the warm hospitality enjoyed during their stay at Los Alamos. Work at Madrid and Leganés has been supported by CICYT (Spain) under project MAT95-0325. Work at Los Alamos is performed under the auspices of the U.S. D.o.E.

[†] Electronic address: diez@dulcinea.uc3m.es

[‡] Electronic address: adame@valbuena.fis.ucm.es

[§] Electronic address: macia@valbuena.fis.ucm.es

^{*} Electronic address: anxo@dulcinea.uc3m.es

¹ R. Merlin, K. Bajema, R. Clarke, F. -Y. Juang, and P. Bhattacharya, Phys. Rev. Lett. **55**, 1768 (1985).

² R. Merlin, K. Bajema, J. Nagle, and K. Ploog, J. Phys. (Paris) Colloq. **48**, C5-503 (1987).

³ R. Merlin, IEEE J. Quantum Electron. **24**, 1791 (1988).

⁴ F. Laruelle and B. Etienne, Phys. Rev. B **37**, 4816 (1988).

⁵ A. A. Yamaguchi, T. Saiki, T. Tada, T. Ninomiya, K. Misawa, and T. Kobayashi, Solid State Commun. **75**, 955 (1990).

⁶ D. Toet, M. Potemski, Y. Y. Wang, J. C. Maan, L. Tapfer, and K. Ploog, Phys. Rev. Lett. **66**, 2128 (1991).

⁷ K. Hirose, D. Y. K. Ko, and H. Kamimura, J. Phys.: Condens. Matter **4**, 5947 (1992).

⁸ D. Munzar, L. Boćáček, J. Humlíček, and K. Ploog, J. Phys.: Condens. Matter **6**, 4107 (1994).

⁹ E. Maciá, F. Domínguez-Adame, and A. Sánchez, Phys. Rev. B **49**, 9503 (1994).

¹⁰ F. Domínguez-Adame, E. Maciá, B. Méndez, Phys. Lett. A **194**, 184 (1994).

¹¹ F. Domínguez-Adame, E. Maciá, B. Méndez, C. L. Roy and A. Khan, Semicond. Sci. Technol. **10**, 797 (1995).

¹² M. Kohmoto, L. P. Kadanoff, and C. Tang, Phys. Rev. Lett. **50**, 1870 (1983).

¹³ C. S. Ryu, G. Y. Oh, and M. H. Lee, Phys. Rev. B **48**, 132 (1993).

¹⁴ F. Bloch, Z. Phys. **52**, 555 (1928); C. Zener, Proc. R. Soc. London Ser. A **145**, 523 (1934).

¹⁵ M. Dignam, J. E. Sipe, and J. Shah, Phys. Rev. B **49**, 10502 (1994).

¹⁶ K. Leo, P. Haring, F. Brüggemann, R. Schwedler, and K. Köhler, Solid State Commun. **84** 943 (1992).

¹⁷ J. Feldmann, K. Leo, J. Shah, D. A. B. Miller, J. E. Cunningham, T. Meier, G. von Plessen, A. Schulze, P. Thomas, and S. Schmitt-Rink, Phys. Rev. B **46**, 7252 (1992).

¹⁸ G. von Plessen and P. Thomas, Phys. Rev. B **45**, 9185 (1992).

- ¹⁹ K. A. Mäder, L. -W. Wang, and A. Zunger, J. Appl. Phys. **78**, 6639 (1995).
²⁰ E. Maciá and F. Domínguez-Adame, Phys. Rev. Lett. **76**, 2597 (1996).
²¹ See W. H. Press, B. P. Flannery, S. A. Teukolsky, and W. T. Wetterling, *Numerical Recipes* (Cambridge University Press, NY, 1986).
²² A. M. Bouchard and M. Luban, Phys. Rev. B **52**, 5105 (1995).
²³ F. Domínguez-Adame, A. Sánchez, and E. Diez, Phys. Rev. B **50**, 17 736 (1994).
²⁴ E. Maciá, F. Domínguez-Adame, and A. Sánchez, Phys. Rev. E **50**, R679 (1994).
²⁵ E. Maciá and F. Domínguez-Adame Semicond. Sci. Technol. (in press, [cond-mat/9604141](#)).
²⁶ P. E. de Brito, C. A. A. da Silva, and H. N. Nazareno, Phys. Rev. B **51**, 6096 (1995).
²⁷ F. Domínguez-Adame and E. Maciá, Phys. Lett. A **200**, 69 (1995).

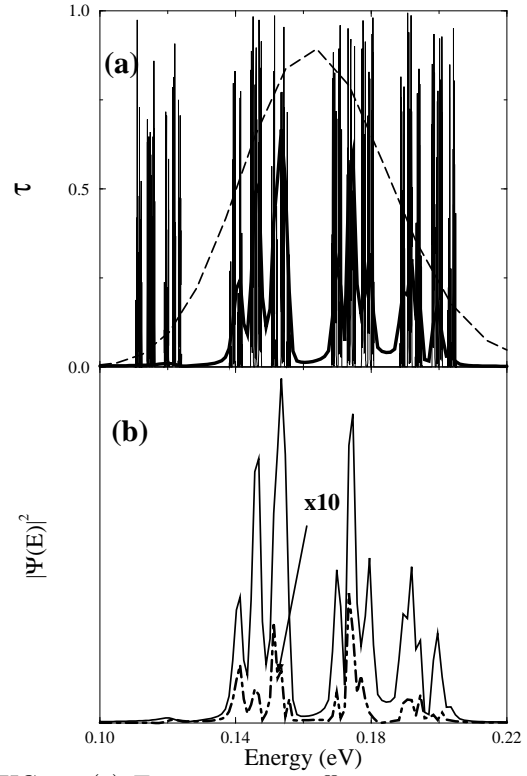


FIG. 2. (a) Transmission coefficient versus incoming energy for a GaAs-Ga_{0.65}Al_{0.35}As FSL with $N = 144$ wells (thin solid line). Fourier transforms of the initial wavepacket ($\Delta X = 200$ Å and $\langle E \rangle = 0.160$ eV, dashed line) and the transmitted wavepacket for perfect FSL ($W = 0$, thick solid line) at $t = 6$ ps are also shown in arbitrary units. (b) Fourier transforms of the transmitted wavepackets for a perfect ($W = 0$, solid line) and imperfect ($W = 0.05$, dashed line) FSLs at $t = 6$ ps. Notice in (a) the perfect coincidence between the filtered wavepacket and the allowed minibands. Parameters are $a = b = 32$ Å and $a' = 26$ Å.

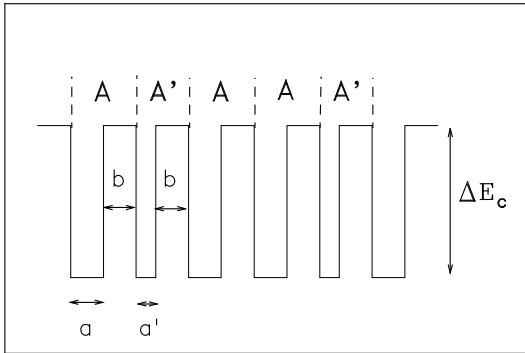


FIG. 1. Schematic diagram of the conduction-band edge of the GaAs-Ga_{1-y}Al_yAs Fibonacci superlattice.

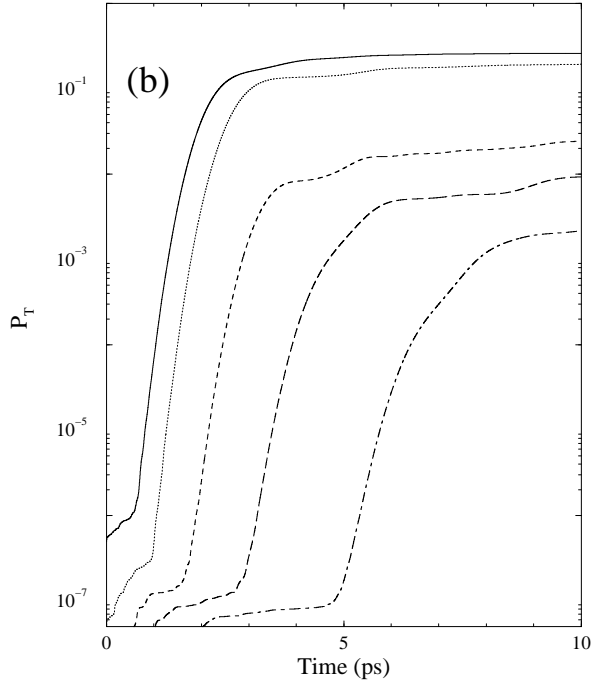
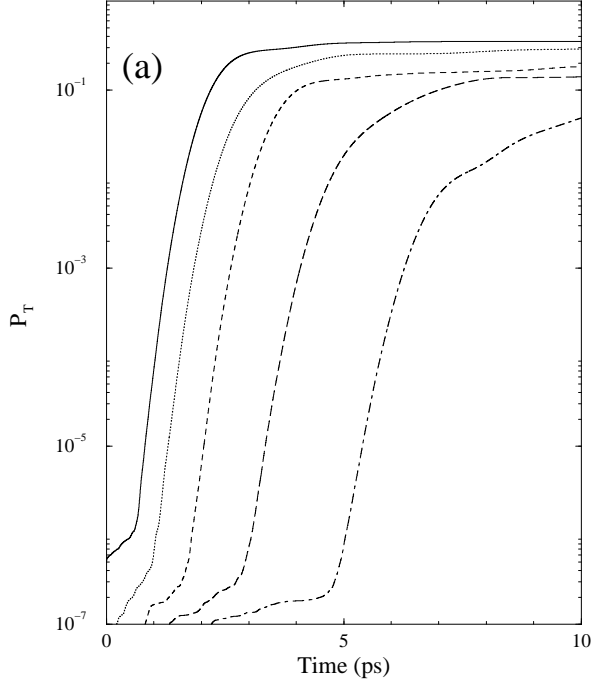


FIG. 3. Transmission probability versus time for (a) perfect $W = 0$ and (b) imperfect $W = 0.05$ GaAs-Ga_{0.65}Al_{0.35}As FSL with various number of wells: From top to bottom $N = 34, 55, 89, 144, 233$. Other parameters are the same as in Fig. 2

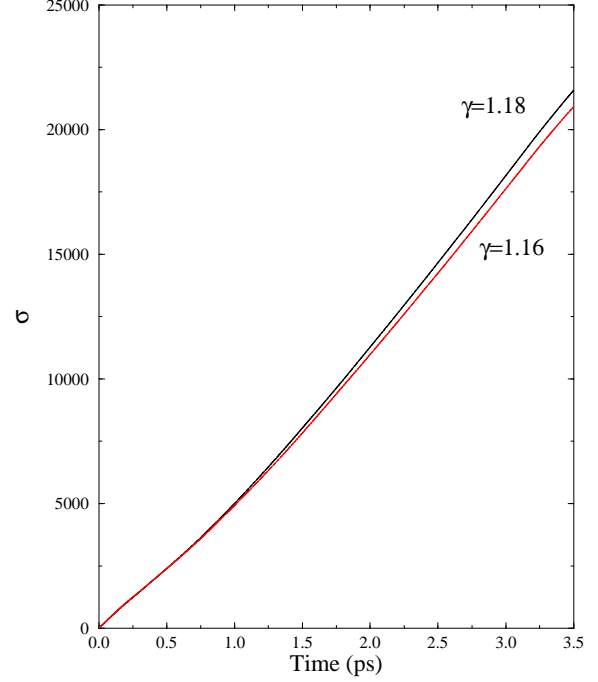


FIG. 4. Mean-square displacement versus time for perfect ($W = 0$, solid line) and imperfect ($W = 0.05$, dashed line) GaAs-Ga_{0.65}Al_{0.35}As FSL with $N = 377$ wells. Other parameters are the same as in Fig. 2. The mean-square displacement grows in time as a power law $\sim t^\gamma$.

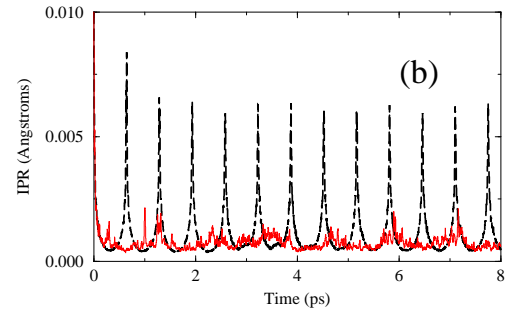
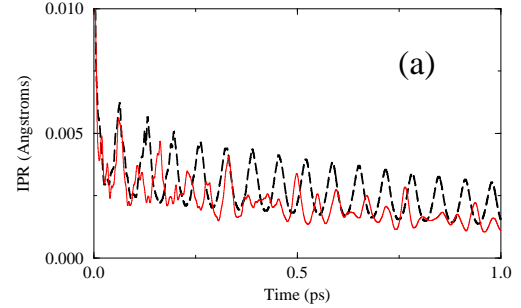


FIG. 5. Inverse participation ratio as function of time for an initial Gaussian wavepacket placed in periodic (dashed line) and Fibonacci (solid line) GaAs-Ga_{0.65}Al_{0.35}As SLs, subject to an electric field (a) $F = 100$ kV/cm and (b) 10 kV/cm. Other parameters are the same as in Fig. 2. The occurrence of Bloch oscillations in the periodic SL is apparent.